Light on the Tip of a Needle: Plasmonic Nanofocusing for Spectroscopy on the Nanoscale

Samuel Berweger, Joanna M. Atkin, Robert L. Olmon, and Markus B. Raschke*

Department of Physics, Department of Chemistry, and JILA, University of Colorado, Boulder, Colorado 80309, United States

ABSTRACT: The efficiency of plasmonic nanostructures as optical antennas to concentrate optical fields to the nanoscale has been limited by intrinsically short dephasing times and small absorption cross sections. We discuss a new optical antenna concept based on surface plasmon polariton (SPP) nanofocusing on conical noble metal tips to achieve efficient far- to near-field transformation of light from the micro- to the nanoscale. The spatial separation of the launching of propagating SPPs from their subsequent apex confinement with high energy concentration enables background-free near-field imaging, tip-enhanced Raman scattering, and nonlinear nanospectroscopy. The broad bandwidth and spectral tunability of the nanofocusing mechanism in combination with frequency domain pulse shaping uniquely allow for the spatial confinement of ultrashort laser pulses and few-femtosecond spatio-temporal optical control on the nanoscale. This technique not only extends powerful nonlinear and ultrafast spectroscopies to the nanoscale but can also generate fields of sufficient intensity for electron emission and higher harmonic generation.
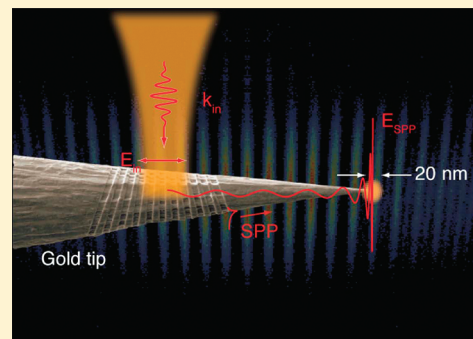
The efficient, reproducible, scalable, and tunable focusing of light into the nanoscale for enhanced spectroscopy and imaging has remained challenging. While in principle the diffraction-limited size of a far-field focus is well matched to the absorption cross section of an ideal resonant dipolar quantum absorber of $3\lambda^2/2\pi$, molecular cross sections are typically limited by nonradiative decoherence via intra- and intermolecular coupling to approximately the geometric size of the molecule.[1] Overcoming this mode mismatch is the goal of using optical antennas, which have evolved from the uncontrolled yet high electromagnetic field enhancement in rough surface-enhanced Raman scattering (SERS) substrates[2] to controllable yet often still inefficient antenna devices to mediate and drive the interaction between free-space light and molecular or nanoscale excitations.[3]

Optical antennas are conceptually analogous to RF antennas. First, a propagating far-field wave is absorbed by the antenna and transduced into a wire-bound and guided electrical current. That antenna current at RF frequencies is then transferred to and converted by the load.[4] However, extension of this concept to optical frequencies is complicated by low electrical conductivities leading to large ohmic losses and the lack of analogous discrete circuit elements preventing optimal impedance matched conditions.

The nascent paradigm for optical antennas has focused on the use of noble metal nanoparticles exhibiting strong polarizabilities at optical frequencies arising from localized SPP resonances. As illustrated in Figure 1a, this in principle enables the transformation of far-field modes with a single free-space wave vector $k_0 = 2\pi/\lambda_0 = \omega_0/c$ into spatially localized evanescent modes with correspondingly large wave vector distributions (red). Through the mode overlap of the large

wavevector distribution with that of the induced molecular point dipole as the load, electromagnetic energy transfer occurs via evanescent dipole–dipole coupling, as illustrated in Figure 1b. The efficiency of this process then depends on the antenna-to-load separation R analogous to, for example, Förster resonant energy transfer (FRET) between two chromophores, with the transfer efficiency proportional to $(1 + (R/R_0)^6)^{-1}$ and typical values of the Förster distance R_0 of a few nanometers, depending on the spectral overlap and relative orientation.[3] Via reciprocity, the reverse process is also facilitated, that is, enhanced radiative antenna-coupled molecular emission.

Due to the high field localization and enhancement generally enabled by localized SPP resonances, optical antennas have found widespread applications for sensing and spectroscopy, most notably in surface-enhanced spectroscopies such as Raman scattering (SERS),[2] infrared absorption (SEIRA),[5] and coherent nonlinear optics such as second-harmonic generation (SHG).[6,7] All-optical imaging with nanometer spatial resolution is enabled by scattering-type scanning near-field optical microscopy (s-SNOM),[8] and its plasmon-enhanced variant tip-enhanced Raman scattering (TERS) can yield single-molecule sensitivity.[9–11] However, despite much progress, significant difficulties persist for lack of a generalizable nanofocusing concept.

While the absorption cross section (effective area) of plasmonic nanoparticles can approach the theoretical limit of RF dipole antennas[4] of $\sigma_{RF,dip} = 0.13\lambda^2$, increasing σ beyond the dipole limit by, for example, increasing the volume of the
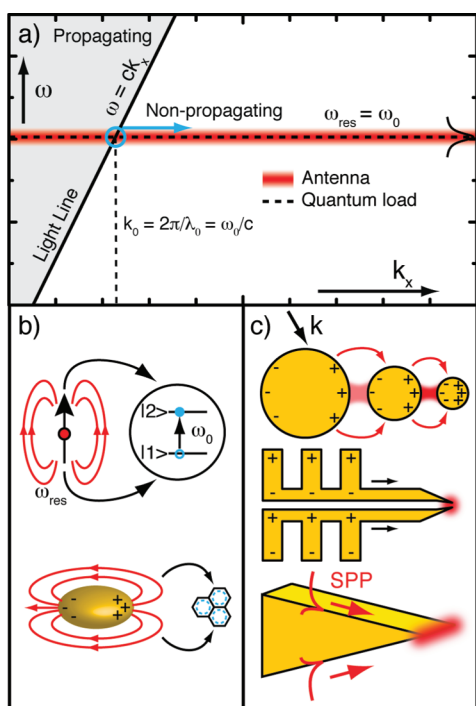
Figure 1. (a) Dispersion relationship of a localized plasmon resonance (optical antenna) and an ideal point dipole (quantum load) at resonance. Using the antenna facilitates the transformation (blue arrow) of a mode consisting of a single free-space wave vector $k_0 = 2\pi/\lambda_0$ into a broad k vector distribution associated with a nanoscopic excitation. (b) Illustration of the near-field dipole−dipole coupling between the antenna and molecular or nanoscale quantum system as the load (top) as well as the specific case of a plasmonic nanoparticle functioning as an antenna (bottom). (c) Different optical antenna concepts for enhanced mode transformation and field localization (see text).

> All-optical imaging with nanometer spatial resolution is enabled by scattering-type scanning near-field optical microscopy. However, despite much progress, significant difficulties persist for lack of a generalizable nanofocusing concept.

plasmonic structure, results in reduced spatial field localization due to smaller associated wave vectors. The intrinsically low Q factors (on the order of 10) arising from short plasmon dephasing times T_2, while providing a broad bandwidth, limit the local field enhancement $F \propto T_2$.[7]

In order to overcome the limited cross sections of single or simple coupled plasmonic nanostructures, gradual mode transformations based on cascaded structures and focusing propagating SPP modes into structural singularities[12] on wedges and grooves[13] have been proposed, as well as the extension of classical antenna concepts such as coplanar strip lines and phased array antennas,[14,15] as illustrated in Figure 1c. While improved performance can be achieved with gradual or multistep mode transformations, the use of resonant structures and nanoparticles remains limited in efficiency due to scattering and radiation losses at the structural discontinuities.

It has long been thought that a 3D regularly tapered conical waveguide could overcome the limitations described above. Its unique topology possesses no structural discontinuities except at the apex, thus minimizing all scattering losses. This allows for a continuous SPP mode transformation, taking advantage of the radius-dependent effective index of refraction ($n_{\text{eff}}(r) \propto 1/r$ for $r \ll \lambda_0$) experienced by SPPs propagating on the outside surface of the structure, as predicted by Babadjanyan et al. in 2000[16] and Stockman in 2004.[17] The increasing index of refraction leads to a decreasing SPP wavelength, thus avoiding scattering loss as the taper narrows, allowing efficient generation of a spatially localized excitation at the waveguide terminus.

In general, the dispersion relationship of an SPP is $k_{\text{SPP}} = k_0 n_{\text{eff}}$, with n_{eff} for the case of a planar or large cylindrical material interface given by

$$n_{\text{eff}} = \sqrt{\frac{\varepsilon_1 \varepsilon_2}{\varepsilon_1 + \varepsilon_2}} \qquad (1)$$

with the dielectric function of the metal and the surrounding dielectric, ε_1 and ε_2, respectively.[18] For $\text{Re}(\varepsilon_1) < 0$ and $|\text{Re}(\varepsilon_1)| > 1$, as is the case for noble metals over a broad frequency range up to the visible spectrum,[19] $k_{\text{SPP}} > k_0$; that is, momentum conservation prevents the coupling of SPPs to free-space light and the SPP wave remains surface-confined. However, $\text{Im}(\varepsilon_1) > 0$, thus $\text{Im}(k_{\text{SPP}}) > 0$ results in appreciable ohmic loss and SPP propagation attenuation.

For a radially symmetric ($m = 0$) mode propagating on a cylindrical waveguide of radius r, $n_{\text{eff}}(r)$ can be calculated by solving the transcendental equation[17,20,21]

$$\frac{\varepsilon_1}{\kappa_1} \frac{I_1(k_0 \kappa_1 r)}{I_0(k_0 \kappa_1 r)} + \frac{\varepsilon_2}{\kappa_2} \frac{K_1(k_0 \kappa_2 r)}{K_0(k_0 \kappa_2 r)} = 0 \qquad (2)$$

with the modified Bessel functions I_j and K_j ($j = 0, 1$) and $\kappa_i = (n_{\text{eff}}^2(r) - \varepsilon_i)^{1/2}$. While higher-order ($m = 1, 2, 3, ...$) asymmetric mode solutions also exist, they do not experience the diverging $n_{\text{eff}}(r)$ with decreasing r necessary for nano-focusing.[22] Instead, these modes have a mode-number-dependent cutoff radius beyond which they cannot propagate.[23]

Shown in Figure 2a are the SPP dispersion relationships calculated from eq 2 using Drude parameters for Au[19] and air as the surrounding dielectric for different cone radii. It can be seen that for all radii, the SPP wave vector k_{SPP} is larger than that of light in free space, with k vectors increasing with decreasing radius. Figure 2b shows the increase in $n_{\text{eff}}(r)$ (green) for the $m = 0$ mode calculated from eq 2 for the case of $\lambda_0 = 633$ nm and a cone half-angle of $\theta = 3.5°$ as an example. Associated with the divergence of $n_{\text{eff}}(r)$ is a decrease in the group velocity $v_g = \partial\omega/\partial k$ (light blue). This gives rise to a decrease in λ_{SPP}, as seen in the spatial evolution of the surface electric field down the cone, calculated from ref 17 and taking into account propagation damping (red). Concomitantly, the index of refraction increase leads to a decrease of the spatial extent of the evanescent SPP field into the dielectric medium, given by $1/\text{Im}(2k_{\text{SPP},r})$ (dark blue). This increases the spatial confinement of the mode on the waveguide. Together, these effects lead to the concentration of the electric field into the cone apex, as seen in the rising electric field amplitude.

For a conical waveguide, the adiabatic parameter $\delta = |d(k_{\text{SPP}})^{-1}/dr| \tan(\theta)$ provides a measure of the rate of change of the plasmon wave vector during propagation. For the adiabatic condition $\delta \ll 1$, the cone angle θ is small, and the gradual change in k_{SPP} minimizes non-ohmic losses. Under this
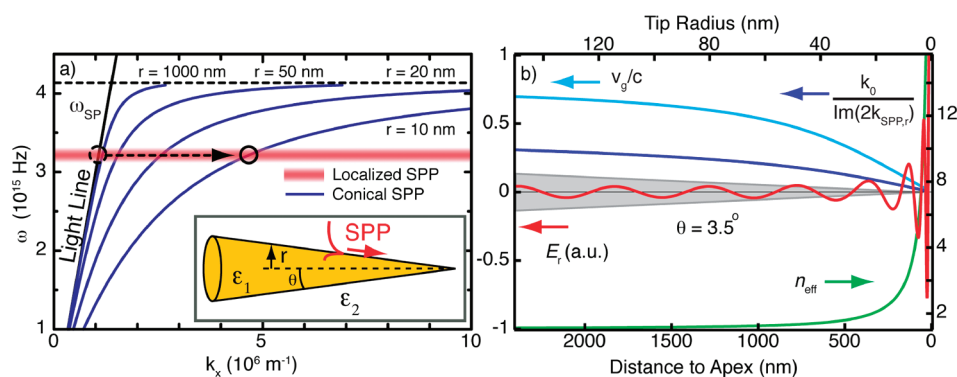
Figure 2. (a) Dispersion relationship for SPPs propagating on a cylindrical waveguide with the radius indicated. The resulting continuous transformation of SPPs propagating on a tapered waveguide presents a highly efficient antenna concept. Upon concentration of the optical field into the tip apex, the propagating mode is converted into a localized mode. (b) Normalized radial electric field at the waveguide surface (red), $n_{eff}(r)$ (green), v_g (light blue), and spatial extent of the electric field outside of the tip normalized to the free-space wavelength (dark blue) as a function of waveguide radius and distance to the apex for a tip with a cone half-angle of $\theta = 3.5°$ and a wavelength of $\lambda_0 = 633$ nm.

condition, the decrease in λ_{SPP} with the change in radius is such that local translational invariance is nearly preserved and scattering losses of the SPP are avoided. However, the greater portion of the SPP field penetrating into the waveguide at smaller radii and the decrease in group velocity during propagation lead to an unavoidable increase in the ohmic loss in the metal. Because small cone angles experience stronger mode confinement over longer propagation distances, the optimal value for θ requires a compromise between reducing ohmic and non-ohmic losses. The competition between these two effects leads to a wavelength-dependent taper angle for optimum energy delivery to the waveguide apex.[24,25] However, the increase in δ near the tip apex[17] may lead to a breakdown of the adiabatic condition.

> The continuous SPP mode transformation taking advantage of a radius-dependent index of refraction experienced by SPPs propagating on the outside of a conical tip leads to nanofocusing at the apex.

In the experimental implementation of 3D SPP nanofocusing, considerations arise in terms of the choice of waveguide fabrication method and the SPP launching mechanism used. Conical tips with smooth surfaces and uniform taper angles, such as those used in scanning probe applications, can be obtained by electrochemical etching from bulk wire.[26] This approach requires attention to surface roughness, which can be minimized through the use of thermal annealing to improve wire crystallinity. Alternatively, tips grown with electron-beam-induced chemical vapor deposition are also suitable but are more time- and equipment-intensive to fabricate.[21] Other approaches, for example, utilizing template-stripping procedures, have also been demonstrated to result in very low surface roughness.[27] The surface roughness is of particular concern as losses can emerge even for nanometer roughness due to scattering and modifications of n_{eff} leading to increased ohmic damping.[18]

Au is the most commonly used material, primarily due to the ambient stability of the metal and the ease of tip fabrication. However, in Au, SPP propagation is associated with high losses near the resonant interband transition, which become especially pronounced for photon energies above ~2 eV.[19] Using Ag as a waveguide material allows for low propagation losses and therefore higher nanofocusing efficiencies,[21] but electrochemical etching methods are not well-established, and structures degrade rapidly under ambient conditions.

In order to overcome the momentum mismatch discussed above and launch SPPs onto tips, the traditional methods of grating coupling or attenuated total internal reflection (ATR) can be used,[18] as well as photonic crystal elements[21] or coupling from dielectric waveguides. The use of prism-based ATR coupling elements has thus far remained impractical due to the geometric constraints of micrometer-scale SPP waveguides.[28] While end-on coupling between dielectric and plasmonic waveguides can in principle be highly efficient,[29] this remains difficult in 3D structures due to the high positioning accuracy required at visible frequencies, and alternative methods such as coupling to SPP modes of a metallic cladding on a tapered waveguide suffer from poor mode overlap.[30] The use of a photonic crystal cavity to localize and couple SPPs onto the base of a tip allows for a transmission-type geometry with facile alignment, but this suffers from residual hole array transmission and far-field radiation superimposed with the apex field.[21,31] In contrast, grating coupling elements can readily be fabricated via focused ion beam milling (FIB) onto the shaft of nanofocusing waveguides,[32] and large theoretical coupling efficiencies are possible.[33]

For ease of fabrication, initial experimental verification of the nanofocusing process was performed on etched Au tips using side-illumination grating coupling.[32] A SEM image of an electrochemically etched Au tip with plasmonic grating is shown in Figure 3a. Superimposed is an optical image showing the illumination of the grating with a far-field focus for launching SPPs which then propagate nonradiatively along the shaft of the tip. The subsequent SPP focusing is seen from the localized emission with the point spread function centered at the apex. With the broken symmetry in the axial direction, the purely evanescent propagating SPPs are converted into a localized radiative SPP at the apex. While the minimization of propagation-induced losses favors short grating–apex separation distances, optimization of the optical alignment and grating coupling conditions benefits from a minimum distance in the 10–20 μm range, depending on application.

The apex-emitted light follows a $\cos^2(\theta)$ polarization dependence, as expected for a nanoscopic dipolar emitter
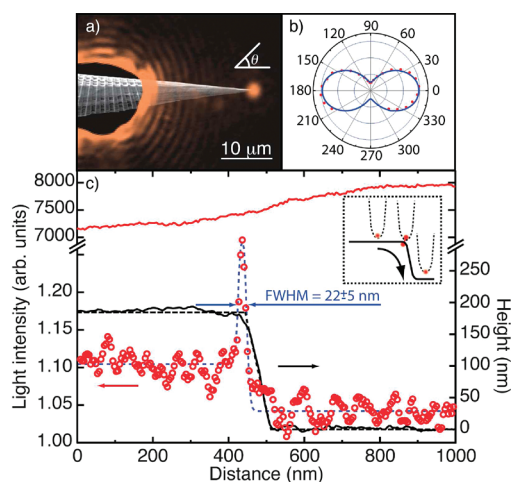
Figure 3. (a) SEM image of an electrochemically etched Au tip with plasmonic grating fabricated via FIB superimposed with an optical image of grating coupling and subsequent reradiation of nanofocused SPPs. (b) Polarization anisotropy of an apex emitter, showing $\cos^2(\theta)$ dependence expected for a subwavelength dipole emitter. (c) Linearly scattered light from the tip as it is scanned over an ultrasharp step edge to determine the emitter size. The shear force topography (black), optical signal (red circles), and fit used to extract fwhm = 22 ± 5 nm (blue) are shown. The red solid line is the elastic scattering measurement acquired with direct apex illumination under otherwise identical conditions. From refs 34 and 35.

located at the tip apex (Figure 3b).[34] These results confirm the expected mode filtering of the nanofocusing process, as only the radially symmetric $m = 0$ SPP mode will produce purely axial dipole emission, due to destructive interference of the radial polarization components.

The degree of spatial confinement at the apex was established in a scanning probe geometry, as shown in Figure 3c, by using an ultrasharp step edge with a 3 nm radius as an effective point scatterer and local probe of the apex field.[34] From the scattering signal, a size of the nanofocus of ~22 ± 5 nm was determined, limited only by the apex size in this case.

Measurements of emitted intensity indicate that 2–4% of the light initially incident on the grating within the coupling bandwidth[34] is re-emitted at the apex of the tip. Despite the high loss during grating coupling and propagation, the confinement of the optical field to a $(20 \text{ nm})^3$ volume at the apex nevertheless represents a power density 2 orders of magnitude higher than a diffraction-limited focus with the same initial intensity.

> The ability to generate a nanoconfined optical excitation at the end of a scanning probe tip with high nanofocusing efficiency holds significant promise for background-free near-field spectroscopy.

The ability to generate a nanoconfined optical excitation at the end of a scanning probe tip with high nanofocusing efficiency holds significant promise for background-free near-field spectroscopy. In conventional s-SNOM implementations, the far-field focus pointed at the tip apex region of the scanning probe tip will often generate a large background, so that demodulation techniques are necessary in order to extract the near-field signal, especially in linear
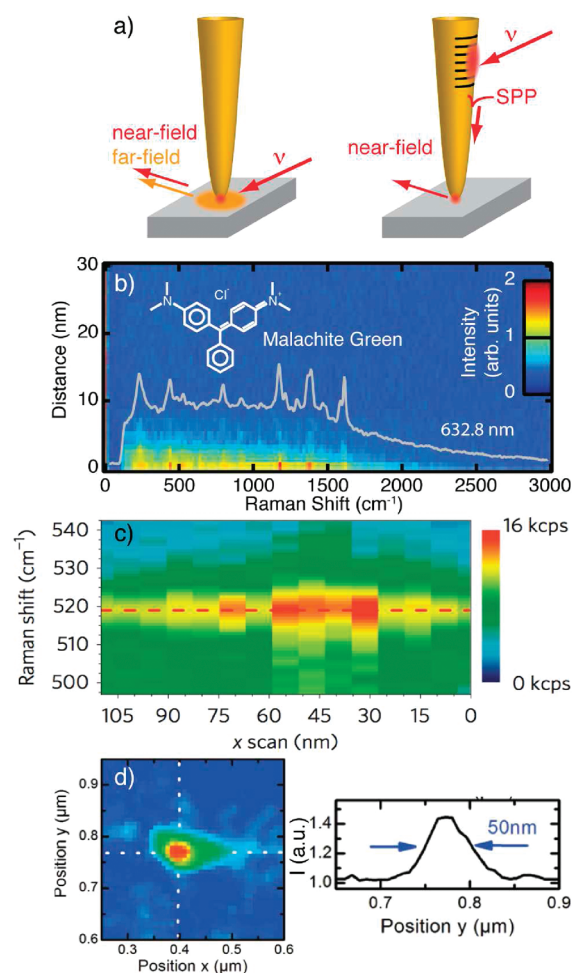
Figure 4. (a) Illustration of the effective far-field background suppression of plasmonic nanofocusing near-field spectroscopy compared to direct far-field illumination of the apex region. (b) Approach curve taken with a grating coupling tip of a monolayer of the dye malachite green on a Au substrate with the resulting TERS spectrum superimposed (gray).[38] The observation of the Raman signal at distances of ~10 nm is a result of the highly confined near-field produced in plasmonic nanofocusing and the effective suppression of the far-field background. (c) TERS of Si with the spectrally resolved line scan taken across a Si edge using photonic crystal tips. Reprinted by permission from Macmillan Publishers Ltd.: Nature Nanotechnology,[21] 2009. (d) Plasmonic nanofocusing linear s-SNOM image acquired from a Au nanoparticle with no background demodulation.[39]

s-SNOM.[36,37] As illustrated in Figure 4a, the spatial separation of SPP launching and apex excitation enabled by plasmonic nanofocusing leads to inherent background suppression.

Initial experiments have demonstrated the application of nanofocusing to TERS[21,38] and elastic light scattering measurements.[39] Figure 4b shows TERS measurements of a monolayer of malachite green deposited onto a Au substrate with 633 nm excitation. While comparable signal levels are observed for plasmonic nanofocusing versus direct illumination, corresponding to a local field enhancement of 20, a complete elimination of the far-field background is achieved using the grating-coupled tips.[38] This demonstrates that the nanofocusing process enables efficient antenna-to-load coupling of the nanofocused point dipole of the source field to the molecular dipole excitation, as discussed above. The extension of TERS to longer wavelengths has long been desirable yet difficult due to

the $1/\lambda^4$ dependence of the Raman scattering intensity. Due to the broad bandwidth of the nanofocusing process and decreased damping at longer wavelengths, however, it is also possible to perform grating-coupled TERS at 785 nm, where the energy concentration and consequently signal levels are found to be 20 times higher than those obtained under identical direct illumination TERS conditions.[38]

Background-free TERS could prove to be particularly useful for the study of crystalline systems, where the far-field Raman background is strong due to the extended material volume probed compared to a molecular monolayer. Shown in Figure 4c is the demonstration of TERS acquired from a Si step using photonic crystal tips.[21] Nanofocusing TERS may thus allow for the full realization of the capabilities of nano-Raman spectroscopy for the study of, for example, strain and domain formation in crystalline or molecular nanocomposite materials on nanometer length scales.

Similarly, spatially resolved background-free imaging using elastic light scattering has been demonstrated recently.[39] As shown in Figure 4d, optical imaging of plasmonic nanoparticles through the interaction between the highly polarizable tip and the particle was performed, thus demonstrating the potential of plasmonic nanofocusing to extend to conventional s-SNOM in cases where low signal levels or low signal-to-noise ratios arise from far-field background contributions. As such, plasmonic nanofocusing s-SNOM is expected to reduce acquisition times through the improved signal-to-noise ratios, as well as increased signal levels from high excitation intensities enabled by increased nanofocusing efficiencies. In general, provided that the excitation intensity remains below the tip and sample damage thresholds, the elimination of the far-field illumination incident on the sample is expected to improve scanning stability and reduces sample bleaching of susceptible resonant systems. In particular, nanofocusing s-SNOM can improve the capabilities of elastic light scattering and vibrational IR nanospectroscopy to image, for example, nanoscale phase separation in correlated electron materials[40] and other spatial inhomogeneities in polymer nanostructures.[41]

> A unique feature of plasmonic nanofocusing on a conical tip is its capability for extension into the time domain.

A unique feature of plasmonic nanofocusing on a conical tip is its capability for extension into the time domain. Previously proposed techniques for spatiotemporal optical control on the nanoscale have relied on the interference of plasmon modes in specially arranged nanoparticle geometries via control of the spectral phase in order to generate localization.[42] This constrained the achievable nanoconfined optical waveforms. In contrast, the nanofocusing mechanism on the tip supports a broad bandwidth with only a weak wavelength dependence and is independent of the spectral phase; it is thus ideal for the nanofocusing and control of ultrafast pulses.

SPP coupling and propagation are expected to give rise to some waveform distortions. These together with the dispersion introduced from the coupling process are predominantly linear,[43] with only small higher-order contributions, and can thus readily be compensated for. The same holds for the SPP propagation- and nanofocusing-induced group delay dispersion (GDD), which can be estimated from $n_{eff}(r,\omega)$ for a tip with

$\theta = 7°$ and a propagation length of 20 μm, yielding a only minimal distortion of the temporal pulse profile with a GDD of < 12 fs^2 before compensation.

It was recently shown that plasmonic nanofocusing in combination with frequency domain pulse shaping allows for the generation of ultrashort pulses in the nanoconfined region of the tip apex, as illustrated in Figure 5a.[35] The high nanofocusing
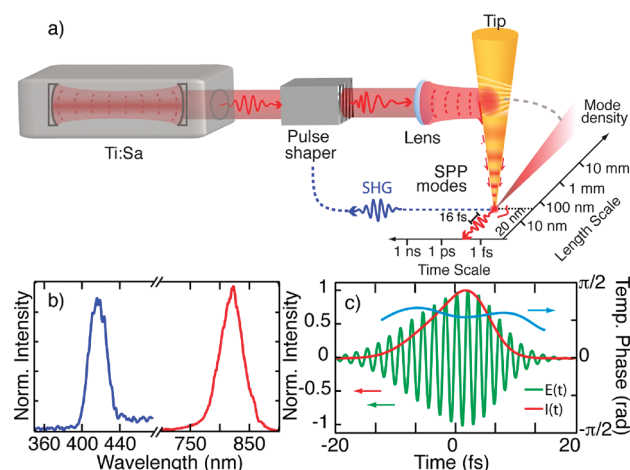
Figure 5. (a) The combination of ultrafast pulse shaping and broadband grating coupling allows for nanofocusing of femtosecond pulses and optical control on the nanoscale. (b) Spectrum showing re-emission of the fundamental nanofocused light and second-harmonic light generated at the apex. (c) Reconstructed femtosecond optical waveform with 16 fs duration and an optical phase as determined by FROG measurement. From ref 35.

efficiency gives rise to local SHG via the broken tip apex symmetry (Figure 5b).[44] As a coherent nonlinear process, this allows for the measurement of the spectral phase of the waveform and serves as a feedback mechanism for pulse optimization and control. Figure 5c shows a nanofocused femtosecond pulse measured at the tip apex with the complete waveform characterized in terms of intensity (red) and phase (blue) by interferometric frequency-resolved optical gating (FROG). After optimization using a multiphoton intrapulse interference phase scan (MIIPS) algorithm, the temporal duration of the pulse with a spectral width of ~60 nm is transform limited at ~16 fs.[35]

With the nanofocusing mechanism being to first order independent of the wavelength and spectral phase, it not only allows for achieving the shortest possible pulse duration but also for generation of arbitrary optical waveforms at the apex through deterministic pulse shaping, with duration only limited by the spectral bandwidth at the apex. For tips exhibiting localized SPP resonances at the apex near the excitation frequencies,[45] plasmon dephasing times of $T_2 \simeq 20$ fs are expected to provide a lower limit for the achievable apex pulse duration.[7] For nonresonant tips, few-femtosecond nanofocusing is possible, as shown recently.[46]

Ultrafast spectroscopy with femtosecond pulses has enabled the study of matter on the characteristic time scales of the elementary electronic and vibrational excitations. Shaping the amplitude and phase of ultrafast pulses allows for coherent control of quantum systems.[42,47] Extension of these techniques to the nanoscale through plasmonic nanofocusing will allow for the all-optical study of the elementary excitations of matter not only on their characteristic time but also on length scales given by electronic and lattice correlations, as shown in Figure 6. Here, the gradual

949

dx.doi.org/10.1021/jz2016268 | *J. Phys. Chem. Lett.* 2012, 3, 945–952
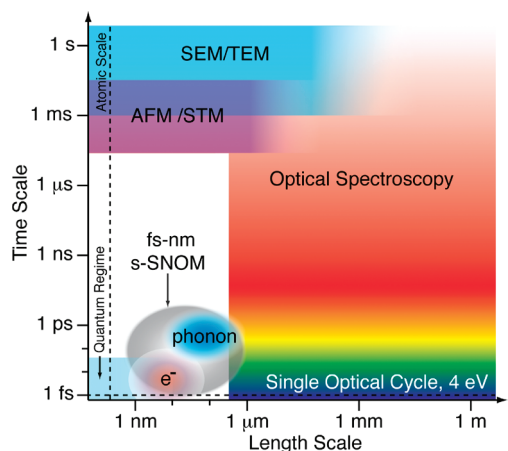
Figure 6. Spatiotemporal regime of the elementary electronic and vibrational excitations in matter as accessible by femtosecond scattering near-field imaging and spectroscopy. Electron and scanning probe microscopies provide access to the quantum regime, but with typically low temporal resolution. Conversely, conventional ultrafast optical spectroscopies are constrained by the diffraction limit and far-field coupling sensitivity.

mode transformation and subsequent antenna transduction into the nanoscale quantum object will overcome sensitivity limits of conventional far-field ultrafast spectroscopy. The approach would complement the related emerging capabilities of ultrafast electron and X-ray imaging. As an all-optical technique, by coupling directly to the electronic and nuclear degrees of freedom, it allows for the study and quantum coherent control of dynamic interactions in molecular and solid matter on the nanoscale and at time scales down to the single-cycle limit.

The use of nanofocusing of SPPs into the nanometer apex of noble metal tips is compatible with implementations of a wide range of spectroscopic techniques. In addition to the improvements gained in TERS and elastic scattering measurements from efficient background suppression, the high nanofocusing efficiency and broad wavelength range allow for the extension of the technique in principle to any wave-mixing process including multidimensional spectroscopies.[6] Furthermore, the high local optical fields that can be generated at the tip apex are sufficient for electron emission via either multiphoton or optical tunneling processes.[48] Strong associated field gradients and optical forces can be used for nanomanipulation and trapping.[49] The control and localization of pulses could also be utilized for higher harmonic generation (HHG) using only high repetition rate Ti:Sa oscillator pulses.[50,51] Although the tip apex is not a true singularity, the diverging index of refraction experienced by surface plasmons is conceptually similar to an event horizon for electromagnetic waves, so that plasmons propagating on a tip may provide a system for modeling related physics.[52]

> Extension of ultrafast spectroscopy to the nanoscale through plasmonic nanofocusing will allow for the all-optical study of the elementary excitations of matter on their characteristic time and length scales simultaneously.

In summary, three-dimensional noble metal tips therefore present a unique waveguide geometry that can be used to transform a grating-coupled quasi-planar SPP mode into a spatially confined excitation for efficient coupling to molecular or nanoscale systems. This antenna concept provides highly efficient generation of nanoconfined excitations with an inherently broad operational bandwidth and only a weak wavelength dependence. In a scanning probe geometry, this allows for nearly background-free s-SNOM imaging with any spectroscopic technique and associated chemical specificity. The combination with ultrafast pulses and frequency domain pulse shaping will allow true nanometer–femtosecond spatiotemporal optical and quantum coherent control.

■ AUTHOR INFORMATION

Corresponding Author
*E-mail: markus.raschke@colorado.edu.

Notes
The authors declare no competing financial interest.

Biographies

Samuel Berweger received his B.S. in physics from the University of California at Santa Cruz in 2006 and a Ph.D. in Physical Chemistry from the University of Washington in 2011. He is currently pursuing ongoing research in the Raschke group as a postdoctoral researcher, with his primary interests on plasmon nanofocusing and related applications.

Joanna M. Atkin received her Ph.D. from Columbia University, working in the Heinz group. She is currently working in the Raschke group as a postdoctoral research assistant with a strong interest in plasmon-enhanced near-field spectroscopy and correlated electron systems.

Robert L. Olmon received a B.S. in Electrical and Computer Engineering from The Ohio State University in 2006, a M.S. in Electrical Engineering in 2009, and a Ph.D. in 2012 from the University of Washington. He is currently a postdoctoral research associate at the University of Colorado in Boulder where he continues his studies of the electromagnetic properties of optical antennas and antenna-coupled systems.

Markus Raschke (Ph.D., Max-Planck Institute for Quantum Optics, 2000) is professor at the University of Colorado, following appointments at the University of California at Berkeley, the Max-Born-Institute in Berlin, and the University of Washington. His research interests are the nanoscale nonlinear and ultrafast spectroscopy of molecular and correlated matter. Website: http://nano-optics.colorado.edu.

■ ACKNOWLEDGMENTS

■ REFERENCES

(1) Mandel, L.; Wolf, E. *Optical Coherence and Quantum Optics*; Cambridge University Press: New York, 1995.
(2) Willets, K. A.; Van Duyne, R. P. Localized Surface Plasmon Resonance Spectroscopy and Sensing. *Annu. Rev. Phys. Chem.* **2007**, *58*, 267.

(3) Novotny, L.; Hecht, B. *Principles of Nano-Optics*; Cambridge: New York, 2006.

(4) Balanis, C. *Antenna Theory: Analysis and Design*; Wiley: New York, 1997.

(5) Osawa, M. *Surface Enahnced Infrared Absorption; Topics in Applied Physics*; Springer: New York, 2001; Vol. 81, p 163.

(6) Canfield, B. K.; Husu, H.; Laukkanen, J.; Bai, B.; Kuittinen, M.; Turunen, J.; Kauranen, M. Local Field Asymmetry Drives Second-Harmonic Generation in Noncentrosymmetric Nanodimers. *Nano Lett.* 2007, 7, 1251.

(7) Anderson, A.; Deryckx, K. S.; Xu, X. G.; Steinmeyer, G.; Raschke, M. B. Few-Femtosecond Plasmon Dephasing of a Single Metallic Nanostructure from Optical Response Function Reconstruction by Interferometric Frequency Resolved Optical Gating. *Nano Lett.* 2010, 10, 2519.

(8) Keilmann, F.; Hillenbrand, R. Near-Field Microscopy by Elastic Light Scattering from a Tip. *Philos. Trans. R. Soc. London, Ser. A* 2004, 362, 787.

(9) Neacsu, C. C.; Dreyer, J.; Behr, N.; Raschke, M. B. Scanning-Probe Raman Spectroscopy with Single-Molecule Sensitivity. *Phys. Rev. B* 2006, 73, 193406.

(10) Zhang, W.; Yeo, B. S.; Schmid, T.; Zenobi, R. Single Molecule Tip-Enhanced Raman Spectroscopy with Silver Tips. *J. Phys. Chem. C* 2007, 111, 1733.

(11) Steidtner, J.; Pettinger, B. Tip-Enhanced Raman Spectroscopy and Microscopy on Single Dye Molecule with 15 nm Resolution. *Phys. Rev. Lett.* 2008, 100, 236101.

(12) Aubry, A.; Lei, D. Y.; Fernandez-Domínguez, A. I.; Sonnefraud, Y.; Maier, S. A.; Pendry, J. B. Plasmonic Light-Harvesting Devices over the Whole Visible Spectrum. *Nano Lett.* 2010, 10, 2574.

(13) Durach, M.; Rusina, A.; Stockman, M. I.; Nelson, K. Toward Full Spatiotemporal Control on the Nanoscale. *Nano Lett.* 2007, 7, 3145.

(14) Krenz, P. M.; Olmon, R. L.; Lail, B. A.; Raschke, M. B.; Boreman, G. D. Near-Field Measurement of Infrared Coplanar Strip Transmission Line Attenuation and Propagation Constants. *Opt. Express* 2010, 18, 21678.

(15) Schnell, M.; Alonso-Gonzalez, P.; Arzubriaga, L.; Casanova, F.; Hueso, L. E.; Chuvilin, A.; Hillenbrand, R. Nanofocusing of Mid-infrared Energy with Tapered Transmission Lines. *Nat. Photonics* 2011, 5, 28.

(16) Babadjanyan, A. J.; Margaryan, N. L.; Nerkararyan, K. V. Superfocusing of Surface Polaritons in the Conical Structure. *J. Appl. Phys.* 2000, 87, 3785.

(17) Stockman, M. I. Nanofocusing of Optical Energy in Tapered Plasmonic Waveguides. *Phys. Rev. Lett.* 2004, 93, 137404.

(18) Raether, H. *Surface Plasmons on Smooth and Rough Surfaces and on Gratings*; Springer-Verlag: New York, 1988.

(19) Johnson, P.; Christy, R. Optical Constants of the Noble Metals. *Phys. Rev. B* 1972, 6, 4370.

(20) Ruppin, R. Effect of Non-locality on Nanofocusing of Surface Plasmon Field Intensity in a Conical Tip. *Phys. Lett. A* 2005, 340, 299.

(21) De Angelis, F.; Das, G.; Candeloro, P.; Patrini, M.; Galli, M.; Bek, A.; Lazzarino, M.; Maksiymov, I.; Liberale, C.; Andreani, L. C.; Di Fabrizio., E. Nanoscale Chemical Mapping Using Three-Dimensional Adiabatic Compression of Surface Plasmon Polaritions. *Nat. Nanotechnol.* 2009, 5, 67.

(22) Baida, F.; Belkhir, A. Superfocusing and Light Confinement by Surface Plasmon Excitation Through Radially Polarized Beam. *Plasmonics* 2009, 4, 51.

(23) Verhagen, E.; Spasenovic, M.; Polman, A.; (Kobus) Kuipers, L. Nanowire Plasmon Excitation by Adiabatic Mode Transformation. *Phys. Rev. Lett.* 2009, 102, 203904.

(24) Issa, N.; Guckenberger, R. Optical Nanofocusing on Tapered Metallic Waveguides. *Plasmonics* 2007, 2, 31.

(25) Gramotnev, D. K.; Vogel, M. W.; Stockman, M. I. Optimized Nonadiabatic Nanofocusing of Plasmons by Tapered Metal Rods. *J. Appl. Phys.* 2008, 104, 034311.

(26) Ren, B.; Picardi, G.; Pettinger, B. Preparation of Gold Tips Suitable for Tip-Enhanced Raman Spectroscopy and Light Emission by Electrochemical Etching. *Rev. Sci. Instrum.* 2004, 75, 837.

(27) Lindquist, N. C.; Nagpal, P.; Lesuffleur, A.; Norris, D. J.; Oh, S.-H. Three-Dimensional Plasmonic Nanofocusing. *Nano Lett.* 2010, 10, 1369.

(28) Sánchez, E. J.; Krug, J. T. II; Xie, X. S. Ion and Electrom Beam Assisted Growth of Nanometric Si_mO_n Structure for Near-Field Microscopy. *Rev. Sci. Instrum.* 2002, 73, 3901.

(29) Chen, X.-W.; Sandoghdar, V.; Agio, M. Highly Efficient Interfacing of Guided Plasmons and Photons in Nanowires. *Nano Lett.* 2009, 9, 3756.

(30) Janunts, N.; Baghdasaryan, K.; Nerkararyan, K.; Hecht, B. Excitation and Superfocusing of Surface Plasmon Polaritons on a Silver-Coated Optical Fiber Tip. *Opt. Commun.* 2005, 253, 118.

(31) De Angelis, F.; Patrini, M.; Das, G.; Maksymov, I.; Galli, M.; Businaro, L.; Andreani, L. C.; Di Fabrizio, E. A Hybrid Plasmonic–Photonic Nanodevice for Label-Free Detection of a Few Molecules. *Nano Lett.* 2008, 8, 2312.

(32) Ropers, C.; Neacsu, C.; Elsaesser, T.; Albrecht, M.; Raschke, M.; Lienau, C. Grating-Coupling of Surface Plasmons onto Metallic Tips: A Nanoconfined Light Source. *Nano Lett.* 2007, 7, 2784.

(33) Baron, A.; Devaux, E.; Rodier, J.-C.; Hugonin, J.-P.; Rousseau, E.; Genet, C.; Ebbesen, T. W.; Lalanne, P. Compact Antenna for Efficient and Unidirectional Launching and Decoupling of Surface Plasmons. *Nano Lett.* 2011, 11, 4207.

(34) Neacsu, C. C.; Berweger, S.; Olmon, R. L.; Saraf, L. V.; Ropers, C.; Raschke, M. B. Near-Field Localization in Plasmonic Super-focusing: A Nanoemitter on a Tip. *Nano Lett.* 2010, 10, 592.

(35) Berweger, S.; Atkin, J. M.; Xu, X. G.; Olmon, R. L.; Raschke, M. B. Femtosecond Nanofocusing with Full Optical Waveform Control. *Nano Lett.* 2011, 11, 4309.

(36) Hillenbrand, R.; Keilmann, F.; Hanarp, P.; Sutherland, D. S.; Aizpurua, J. Coherent Imaging of Nanoscale Plasmon Patterns with a Carbon Nanotube Optical Probe. *Appl. Phys. Lett.* 2003, 83, 368.

(37) Jones, A. C.; Olmon, R. L.; Skrabalak, S. E.; Wiley, B. J.; Xia, Y. N.; Raschke, M. B. Mid-IR Polasmonics: Near-Field Imaging of Coherent Plasmon Modes of Silver Nanowires. *Nano Lett.* 2009, 9, 2553.

(38) Berweger, S.; Atkin, J. M.; Olmon, R. L.; Raschke, M. B. Adiabatic Tip-Plasmon Focusing for Nano-Raman Spectroscopy. *J. Phys. Chem. Lett.* 2010, 1, 3427.

(39) Sadiq, D.; Shirdel, J.; Lee, J. S.; Selishcheva, E.; Park, N.; Lienau, C. Adiabatic Nanofocusing Scattering-Type Optical Nanoscopy of Individual Gold Nanoparticles. *Nano Lett.* 2011, 11, 1609.

(40) Qazilbash, M. M.; Brehm, M.; Chae, B.-G.; Ho, P.-C.; Andreev, G. O.; Kim, B.-J.; Yun, S. J.; Balatsky, A. V.; Maple, M. B.; Keilmann, F.; Kim, H.-T.; Basov, D. N. Mott Transition in VO_2 Revealed by Infrared Spectroscopy and Nano-Imaging. *Science* 2007, 318, 1750.

(41) Raschke, M. B.; Molina, L.; Elsaesser, T.; Kim, D. H.; Knoll, W.; Hinrichs, K. Apertureless Near-Field Vibrational Imaging of Block-Copolymer Nanostructures with Ultrahigh Spatial Resolution. *ChemPhysChem* 2005, 6, 2197.

(42) Aeschlimann, M.; Bauer, M.; Bayer, D.; Brixner, T.; Cunovic, S.; Dimler, F.; Fischer, A.; Pfeiffer, W.; Rohmer, M.; Schneider, C.; Steeb, F.; Strüber, C.; Voronine, D. V. Spatiotemporal Control of Nanoptical Excitations. *Proc. Natl. Acad. Sci. U.S.A.* 2010, 107, 5329.

(43) Yalcin, S. E.; Wang, Y.; Achermann, M. Spectral Bandwidth and Phase Effects of Resonantly Excited Ultrafast Surface Plasmon Pulses. *Appl. Phys. Lett.* 2008, 93, 101103.

(44) Neacsu, C. C.; Reider, G. A.; Raschke, M. B. Second-Harmonic Generation from Nanoscopic Metal Tips: Symmetry Selection Rules for Single Asymmetric Nanostructures. *Phys. Rev. B* 2005, 71, 201402.

(45) Neacsu, C. C.; Steudle, G. A.; Raschke, M. B. Plasmonic Light Scattering from Nanoscopic Metal Tips. *Appl. Phys. B: Laser Opt.* 2005, 80, 295.

(46) Sadiq, D.; Shirdel, J.; Vasa, P.; Lienau. C.; *Proceedings of the 5th International Conference on Surface Plasmon Photonics*, Busan, Korea, May 15–20, 2011; and private communication with C. Lienau.

(47) Kubo, A.; Onda, K.; Petek, H.; Sun, Z.; Jung, Y. S.; Kim, H. K. Femtosecond Imaging of Surface Plasmon Dynamics in a Nano-structured Silver Film. *Nano Lett.* **2005**, *5*, 1123.

(48) Ropers, C.; Solli, D. R.; Schulz, C. P.; Lienau, C.; Elsaesser, T. Localized Multiphoton Emission of Femtosecond Electron Pulses from Metal Nanotips. *Phys. Rev. Lett.* **2007**, *98*, 043907.

(49) Juan, M. L.; Righini, M.; Quidant, R. Plasmon Nano-Optical Tweezers. *Nat. Photonics* **2011**, *5*, 349.

(50) Krüger, M.; Schenk, M.; Himmelhoff, P. Attosecond Control of Electrons Emitted from a Nanoscale Tip. *Nature* **2011**, *475*, 78.

(51) Park, I. Y.; Choi, S. K. J.; Lee, D. H.; Kim, Y. J.; Kling, M. F.; Stockman, M. I.; Kim, S. W. Plasmonic Generation of Ultrashort Extreme-Ultraviolet Light Pulses. *Nat. Photonics* **2011**, *5*, 677.

(52) Smolyaninov, I. I.; Davis, C. C. Linear and Nonlinear Optics of Surface-Plasmon Whispering-Gallery Modes. *Phys. Rev. B* **2004**, *69*, 205417.